

Structural complementarity and similarity: linking relational principles to network structure

Szymon Talaga^{1*}

Andrzej Nowak^{2,3}

¹Robert Zajonc Institute for Social Studies, University of Warsaw,
Stawki 5/7, 00-183 Warsaw, Poland.

²Faculty of Psychology, University of Warsaw,
Stawki 5/7, 00-183 Warsaw, Poland.

³Department of Psychology, Florida Atlantic University,
777 Glades Rd, Boca Raton, FL 33431, USA.

*Corresponding author; E-mail: stalaga@uw.edu.pl

Abstract

Similarity is one of the most important relational principles shaping the structure of networks. It is linked to homophily, triadic closure and the abundance of triangles as its characteristic motif. However, many important phenomena, such as collaboration and division of labor, are driven rather by complementarity, or differences and synergy. The principle of complementarity attracted much less attention and in particular has not been operationalized in network terms. Here we address this problem and show that complementarity is linked to the abundance of quadrangles and the presence of dense bipartite-like subgraphs. Starting from very general geometric arguments we define two families of coefficients: (1) similarity coefficients generalizing the notions of local clustering and closure; (2) analogous complementarity coefficients based on quadrangles instead of triangles. We study their main properties and behavior in random graph models and demonstrate their theoretical validity and practical utility on a set of real-world social networks. We show that friendship relations are linked to increased levels of structural similarity and health advice to significantly higher complementarity.

Keywords — similarity, complementarity, homophily, heterophily, structural equivalence, network geometry

1. Introduction

The structure of networks is commonly indicative of their functional properties as well as mechanisms or processes that created them. It is one of the important insights of network science that the statistical overrepresentation of particular motifs (small subgraphs) is very often informative of the underlying generating processes or functional properties of a given system [41]. In particular, there is a large body of evidence showing that the abundance of triangles (3-cycles) is a structural signature of relations driven by similarity between nodes in some (possibly latent) metric space [9, 10, 12, 32, 50].

The importance of similarity and its impact on structure of social networks has been recognized in sociology for a long time, as it is linked to homophily and triadic closure [5, 31, 37, 40, 46]. While

it is usually hard to disentangle their effects [4], these two processes are also inherently linked as they lead to structural similarity between connected nodes. In other words, in similarity-driven systems two adjacent nodes are likely to share a lot of neighbors, and this implies the abundance of triangles and a latent geometric structure [32, 44].

Geometry induced by similarity has been often used for defining statistical models of social networks [26, 33], as well as networks from other domains, including protein-protein interaction and brain networks [3, 25] or the Internet [11]. Moreover, geometric representations of social systems have a long tradition in sociology [8, 13, 14, 39].

However, while important, similarity cannot be the only relational principle organizing the structure of networks. For instance, some phenomena such as cooperation, consumer choices, some types of protein-protein bindings or business interactions and division of labor may be better explained by complementarity or synergy between diverse features of the participating agents [17, 19, 21, 36, 48, 51, 56]. More generally, complementarity can be seen as a particular interpretation of the principle of heterophily, which is a preference for connecting to others who are different with respect to some salient attributes [48].

Hence, it is natural to ask whether there are motifs characteristic for complementarity-driven relations, in the same way as triangles are characteristic for similarity? And whether there is some latent geometric principle that would explain it? This problem of structural signatures of complementarity and their geometric interpretation has attracted much less attention than similarity, but it is no less fundamental and needs to be addressed.

In this paper we introduce a simple but comprehensive approach for quantifying the extent to which relations in networks are driven by the relational principles of similarity and complementarity. To do so, we define two families of graph-theoretical coefficients which are based on the idea of linking relational principles to their characteristic network motifs. The coefficients are purely combinatorial but are derived from first principles based on very general geometric arguments.

We start from the simpler case of similarity coefficients which can be seen as a generalization of local clustering and closure coefficients [55, 57]. They are based on linking the principle of similarity to the abundance of triangles as its characteristic motif and can be defined for edges, nodes and entire graphs. Then, starting from a simple geometric model we argue that quadrangles (4-cycles) are the characteristic motif for complementarity and use the same logic as in the case of similarity to define an analogous family of complementarity coefficients. Crucially, our approach allows us to show that complementarity is inherently linked to the presence of locally-dense bipartite-like subgraphs.

We will call the proposed measures *structural coefficients* because they will not be defined with respect to node attributes, latent or observed, but to how different nodes are embedded in the network and connected to their 1- and 2-hop neighbors. Moreover, we will show that they are closely linked to the fundamental notion of structural equivalence [42, 54].

In the second part of the paper we study the behavior of structural coefficients in some of the most fundamental random graph models as well as several real-world networks from different domains. In particular, we focus on correlations with node degrees. Then, we demonstrate the theoretical validity and practical utility of the proposed framework and show that structural coefficients can be used to effectively discriminate between real-world social networks driven by similarity, or homophily, and complementarity. We end by concluding remarks and a discussion of promising connections to other results.

Last but not least, all methods introduced in this paper are implemented in a Python package called `pathcensus` (see Sec. 4.2). It will be distributed through *Python Package Index* upon publication.

Datasets used and technical details including efficient methods for computing the proposed structural coefficients are discussed in Sec. 4 (Materials and methods) as well as Supplementary Materials (SM). In particular, we discuss an efficient algorithm for counting triples/quadruples and triangles/quadrangles. Summary of the notation used for denoting structural coefficients is presented in Table 1.

1.1. Notation & technical remarks

In this paper we consider simple undirected and unweighted graphs $G = (V, E)$. We use $n = |V|$ and $m = |E|$ to denote numbers of nodes and edges in G respectively. Elements of the adjacency matrix of a graph G will be denoted by a_{ij} and assumed to be equal to 1 if the edge (i, j) exists and 0 otherwise. For any node $i \in V$ we denote its degree by d_i and its k -hop neighborhood by $\mathcal{N}_k(i)$, in particular 1-hop neighborhood will be denoted by $\mathcal{N}_1(i)$. Moreover, we will use $n_{ij} = |\mathcal{N}_1(i) \cap \mathcal{N}_1(j)|$ to denote the number of shared neighbors between nodes i and j . Averaged quantities will be denoted by diamond brackets. For instance, $\langle d_i \rangle$ will denote average node degree.

2. Results

2.1. Structural similarity

It is arguably natural to think about similarity in terms of distance between different objects in a feature space. Hence, the motivating geometric model for similarity-driven relations posits that nodes are positioned in some metric space and the probability of observing a link between them is a decreasing function of the corresponding distance. Such a generic model can be seen as an instance of the class of Random Geometric Graphs (RGGs) [10, 50]. The crux is that this very general formulation is enough to guarantee the abundance of triangles (3-cycles), provided that the link probability function decreases with respect to distance at a high enough rate [32]. In other words, triangles are the characteristic network motif for similarity-driven relations (see Fig. 1A).

In this light, a natural starting point for our endeavor is *local clustering coefficient* [55], of which value for node i will be denoted by s_i^W . It is a classical network measure of how dense the 1-hop neighborhood (ego-network) of i is and it is defined as:

$$s_i^W = \frac{2T_i}{t_i^W} \quad (1)$$

where T_i is the number of triangles including i and t_i^W is the number of wedge triples centered at i or 2-paths with i in the middle (Fig. 1B). Crucially, $s_i^W \in [0, 1]$ and is equal to 1 if and only if $\mathcal{N}_1(i)$ forms a fully connected network. In sociological terms, it measures the extent to which *my friends are friends with each other*. Note, however, that this is only one side of the triadic closure process as it corresponds to the closing of the loop between friends of the focal node i . The other part is about closing the loop between i and friends of its friends and local clustering coefficient does not capture it.

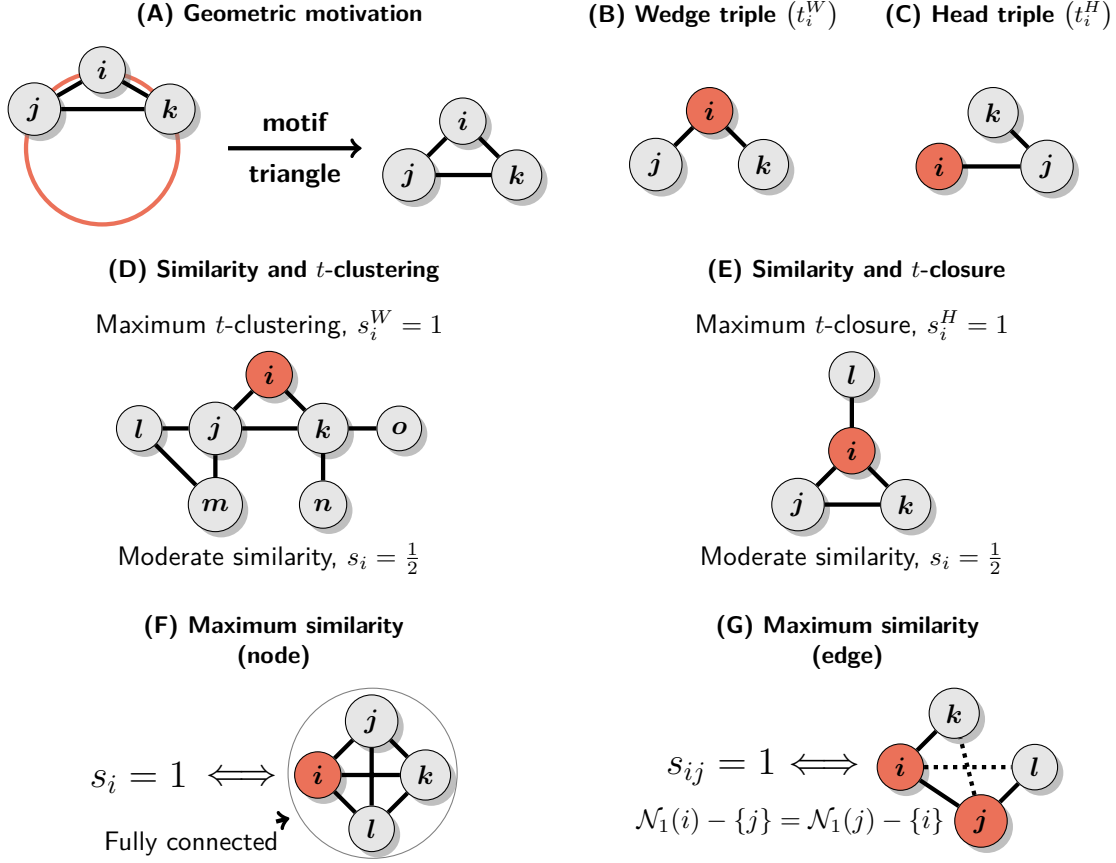


Figure 1. Geometric motivation and the main properties of structural similarity coefficients. (A) Metric structure induced by similarity leads to the abundance of triangles making them its characteristic motif. (B and C) Wedge and head triples. (D) Local clustering can be maximized even when neighbors of the focal node are very differently embedded within the network, while s_i correctly recognizes this fact. (E) Local closure can be maximized even for nodes with sparse 1-hop neighborhoods if they are star-like as neighbors with degree one do not generate any head triples. On the other hand, s_i is sensitive to this deviation from the similarity-driven pattern of connections. (F and G) Necessary and sufficient conditions for maximum structural similarity coefficient at the levels of nodes and edges.

To address this issue a new *local closure coefficient* [57] has been proposed more recently:

$$s_i^H = \frac{2T_i}{t_i^H} \quad (2)$$

where t_i^H is the number of head triples originating from i , that is, 2-paths starting at i (Fig. 1C). It is also in the range of $[0, 1]$ and attains the maximum value if and only if no neighbor of i is adjacent to a node which is not already in $\mathcal{N}_1(i)$. In other words, when $s_i^H = 1$ a random walker starting at i will never leave $\mathcal{N}_1(i)$. Thus, local closure coefficient measures the extent to which

friends of my friends are my friends, that is, it is a measure of the triadic closure between the focal node i and neighbors of its neighbors. As a result, it captures exactly that what local clustering is blind to. Since the local clustering and closure coefficients are based on triples we will later refer to them as t -clustering and t -closure respectively.

The two coefficients complement each other so it is only natural to combine them in a single measure. We now propose such a measure which we will call *structural similarity coefficient*:

$$s_i = \frac{4T_i}{t_i^W + t_i^H} = \frac{t_i^W s_i^W + t_i^H s_i^H}{t_i^W + t_i^H} \quad (3)$$

Note that s_i is equal to the fraction of both wedge and head triples including i which can be closed to make a triangle. It is also equivalent to a weighted average of s_i^W and s_i^H , which implies that $\min(s_i^W, s_i^H) \leq s_i \leq \max(s_i^W, s_i^H)$. Moreover, since $s_i^W = 1$ if and only if $\mathcal{N}_1(i)$ is fully connected and $s_i^H = 1$ if there are no links leaving $\mathcal{N}_1(i)$ then it must be that $s_i = 1$ if and only if i belongs to a fully connected network (Fig. 1F), so in the limit as $s_i \rightarrow 1$ the coefficient becomes a global measure describing the structure of the entire component containing i . Fig. 1 provides a summary of the motivation and main properties of s_i , including examples of when t -clustering and t -closure coefficients are maximal while structural similarity is only moderate (Figs. 1D and 1E).

2.1.1. Edge-wise similarity and structural equivalence

Structural similarity coefficient can also be defined for edges. In this case it is equal to the ratio of triangles including nodes i and j to the total number of 2-paths traversing the (i, j) edge (Fig. 1G). In other words, it is equivalent to the number of shared neighbors relative to the total number of neighbors of i and j , excluding i and j themselves:

$$s_{ij} = \frac{2T_{ij}}{t_{ij}^W + t_{ij}^H} = \frac{2n_{ij}}{d_i + d_j - 2} \quad (4)$$

where T_{ij} is the number of triangles including i and j , t_{ij}^W is the number of (k, i, j) and t_{ij}^H of (i, j, k) triples. Importantly, s_{ij} is symmetric since $T_{ij} = T_{ji}$ and $t_{ij}^W = t_{ji}^H$.

Note that s_{ij} is closely related to the Sørensen Index or normalized Hamming similarity [42, 49], $H_{ij} = 2n_{ij}/(d_i + d_j)$, and differs only in the -2 term in the denominator which accounts for the fact that i and j are known to be connected. Hamming distance/similarity is one of the common measures of structural equivalence [Sec. 7.12.3 in 42] which implies that the proposed node-wise similarity coefficient can be seen as a proxy for the extent to which i is structurally equivalent to its own neighbors. More concretely, since s_i can be expressed as a weighted average of s_{ij} 's for $j \in \mathcal{N}_1(i)$ we have that:

$$\min_j H_{ij} < s_i \leq \max_j \left(H_{ij} \frac{d_i + d_j}{d_i + d_j - 2} \right) \approx \max_j H_{ij} \quad (5)$$

In other words, local similarity coefficient of a node i is approximately bounded between minimum and maximum structural equivalence between i and any of its neighbors (see SM: S1 for the derivation). This justifies the interpretation of the proposed similarity coefficients in terms of *structural similarity*.

2.1.2. Global similarity

From the global perspective both local clustering and local closure lead to the same conclusion that the corresponding global measure is just the fraction of triples that can be closed to make a triangle [57]. This implies that the same quantity is also the proper global measure of the extent to which relations are driven by similarity. In other words, the *global similarity coefficient* is equal to the standard global clustering coefficient and can be defined as:

$$s = \frac{3T}{\sum_i d_i(d_i - 1)} \quad (6)$$

where T is the total number of triangles and the denominator counts the number of triples.

Note that it is indeed a reasonable measure of similarity-driven relations as it is maximized only when a network is fully connected, so all nodes are structurally redundant and can be removed without affecting the overall connectivity.

2.2. Structural complementarity

First, let us consider an intuitive meaning of complementarity. We posit that two objects are complementary when their features are different but in a well-defined synergistic way. As we will see, this additional synergy constraint is crucial. However, before we discuss this further let us note that in the case of similarity an analogous constraint is built-in by design. It is so, because for any point there is always only one point minimizing the distance in the feature space (maximizing similarity) and it is the point itself. Hence, it is arguably natural to say that any object is most similar to itself. As a result, there is a well-defined notion of maximal similarity.

On the other hand, the case of difference is more complex. To make our argument more concrete, let the feature space be \mathbb{R}^k with $k \geq 1$. Now, it is easy to see that for any two points p and r at a distance $d(p, r)$ we can find a third point s such that $d(p, s) > d(p, r)$. In other words, for any point p there is no well-defined point at the maximum distance. As a result, complementarity cannot be defined in terms of difference without some additional constraints. Intuitively, complementarity understood in terms of unconstrained difference inevitably leads to the result that for any object there is an infinite variety of more and more complementary (different) objects, which clearly does not map well on the common understanding of the notion of complementarity. Thus, we need a definition with the same property as in the case of similarity, that is, one yielding a sequence of ever smaller sets of more and more complementary elements converging to a single well-defined point in the limit of maximum complementarity.

Note that the above abstract argument can be related to known complementarity-driven systems in a rather straightforward manner. For instance, a key and a lock are complementary not because they are just different in an arbitrary manner, but because they differ in a very specific way by being structural negatives of each other. Similarly, division of labor in advanced societies is based on complex synergies between capabilities of different individuals and organizations.

Thus, we argue that complementarity should be defined in terms of distance maximization but with additional constraints ensuring that for any point in the feature space there is only one point at the maximum distance. This can be achieved in several different ways, but to keep things simple we will focus on one particularly natural and convenient solution.

We consider nodes as placed on the surface of a k -dimensional (hyper)sphere with $k \geq 1$. In this setting for each point there is only a single point at the maximum distance and the maximum

distance is the same for all points. Now, if nodes connect preferentially to others who are far away, we obtain a model analogous to the similarity but now the connections of a node are not concentrated in its vicinity but instead on the other side of the space. From this it follows that any two connected nodes i and j will not share a lot of neighbors, so triangles will be rare, but instead the 1-hop neighborhood of i should be approximately equal to the 2-hop neighborhood of j and *vice versa*, that is, $\mathcal{N}_1(i) \approx \mathcal{N}_2(j)$ and $\mathcal{N}_2(i) \approx \mathcal{N}_1(j)$. Such a spatial structure must inevitably lead to the abundance of quadrangles and in general locally dense bipartite-like subgraphs (Fig. 2A).

Note that the choice of a (hyper)sphere surface is far from arbitrary as it is a specific instance in the broader class of compact homogeneous and isotropic manifolds, for which it has been shown that it is a proper choice for a latent geometry capable of reproducing jointly sparsity with high clustering, small-world effect and arbitrary degree distributions in similarity-driven networks [10]. In other words, in this setting latent geometry can explain some of the most fundamental structural properties of many real-world networks, in particular social networks [50]. Thus, we argue, it is also a natural first choice for representing relations driven by complementarity, especially that thanks to its structure it seems particularly well-suited for this task (but see Ref. [30] for an alternative approach).

Depending on the context different authors may refer to slightly different objects when using the term *quadrangle*. Namely, a quadrangle may contain up to two chords or diagonal links between its vertices. Here we will consider only quadrangles without any chords which we will call *strong quadrangles*. This choice follows, of course, from the proposed geometric model and the fact that only strong quadrangles are characteristic for locally dense bipartite graphs.

Now we can start defining coefficients measuring complementarity-driven relations. As previously, we begin with a local clustering coefficient which we will call q -clustering. It is defined analogously, but this time in terms of quadrangles and wedge quadruples, that is, 3-paths with the focal node i at the second position (Fig. 2B):

$$c_i^W = \frac{2Q_i}{q_i^W} \quad (7)$$

where Q_i is the number of strong quadrangles including the focal node i and q_i^W is the number of wedge quadruples it belongs to. Note that we consider only quadruples with i at the second position, such as (l, i, j, k) but not (k, j, i, l) , in order to avoid double counting and make the number of wedge and head quadruples per quadrangle equal. Intuitively, it quantifies the extent to which the local environment of i is bipartite-like and its neighbors are structurally equivalent to each other.

Local q -closure coefficient is defined in the same way as the fraction of head quadruples originating from i (Fig. 2C) that can be closed to make a (strong) quadrangle:

$$c_i^H = \frac{2Q_i}{q_i^H} \quad (8)$$

where q_i^H is the number of head quadruples starting at i . Conceptually, it measures the extent to which the local environment of i is bipartite-like and i is structurally equivalent to its 2-hop neighbors.

We can now define *structural complementarity coefficient* as the fraction of quadruples including the focal node i which can be closed to make a (strong) quadrangle which, again, is equivalent to a weighted average of q -clustering and q -closure:

$$c_i = \frac{4Q_i}{q_i^W + q_i^H} = \frac{q_i^W c_i^W + q_i^H c_i^H}{q_i^W + q_i^H} \quad (9)$$

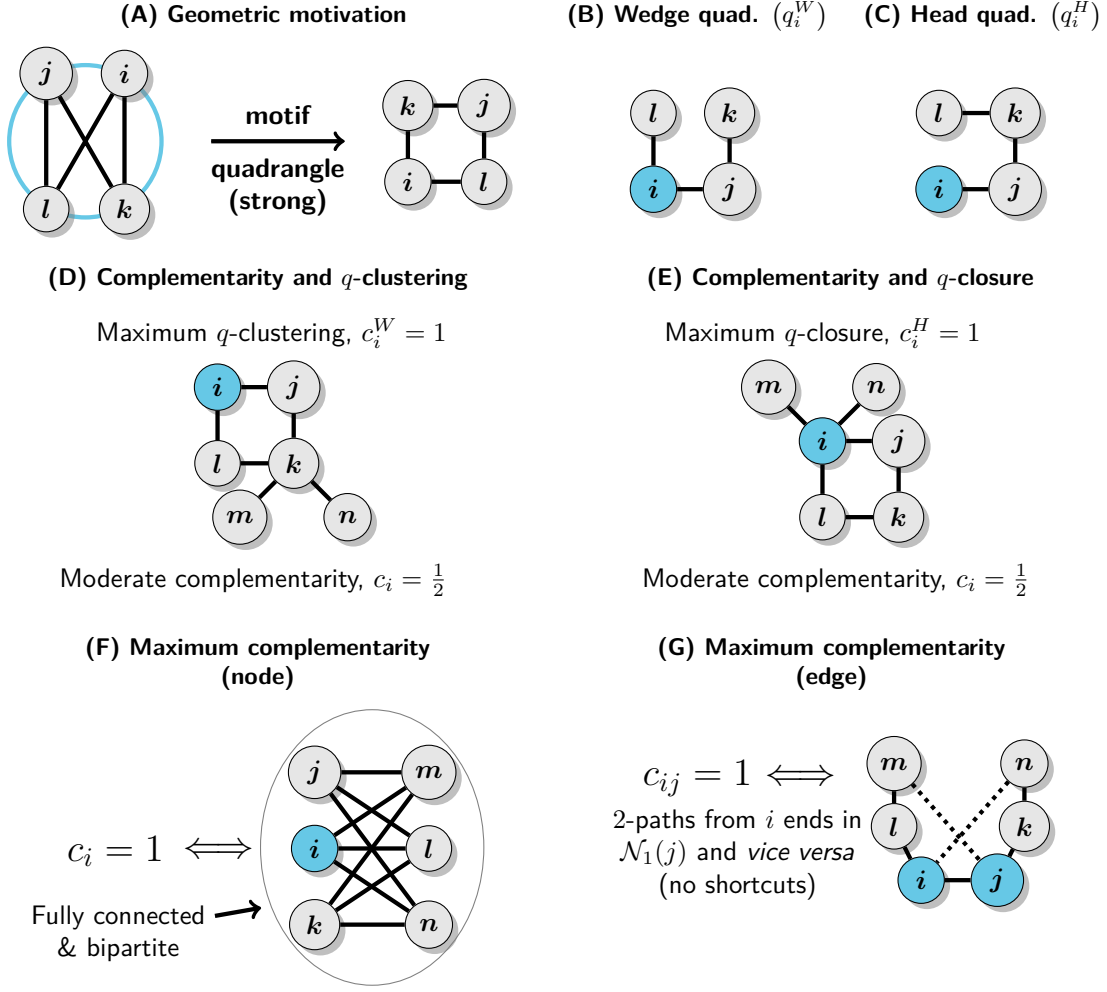


Figure 2. Geometric motivation and the main properties of structural complementarity coefficient. (A) On the surface of a (hyper)sphere for each point there is only a single other point at the maximum distance, so complementarity based on distance maximization must lead to the abundance of (strong or chord-less) quadrangles and locally dense bipartite-like structures. (B and C) Wedge and head quadruples. (D) Local q -clustering can be maximized even when some 2-hop neighbors (node k on the figure) of the focal node connect to nodes which are not in $\mathcal{N}_1(i)$, while the complementarity coefficient correctly identifies this structure. (E) Local q -closure can be maximized even for nodes with sparse 1-hop neighborhoods if they are star-like as neighbors with degree one do not generate any head quadruples. (F and G) Necessary and sufficient conditions for maximum structural complementarity coefficient at the levels of nodes and edges.

Note that again we have that $\min(c_i^W, c_i^H) \leq c_i \leq \max(c_i^W, c_i^H)$, so c_i is always bounded between its constitutive clustering and closure coefficients. Moreover, the interpretations of q -clustering and q -closure jointly imply that $c_i = 1$ if and only if the focal node i belongs to a fully connected bipartite network. Fig. 2 presents a summary of the most important terms and facts related to c_i .

Last but not least, the geometric model underlying the definition of c_i indeed justifies the interpretation in terms of complementarity or synergy. Nodes are more likely to be connected when they are far away in the feature space, meaning that they have different properties which can be possibly combined in a synergistic manner. Crucially, the mesoscopic network structure that is implied by this model is also related to complementarity in a straightforward manner. Bipartite networks are representations of complementarity-driven systems *par excellence* as they consist of two types of nodes and allow only for connections between them. Hence, c_i , being a combined measure of local bipartiteness and density, is actually indicative of the degree to which the local environment of a node resembles such a complementarity-driven system. Note that the fact that c_i is constrained by the density of bipartite connections is crucial as tree-like networks are also locally bipartite-like (i.e. $\mathcal{N}_1(i)$ corresponds to the first type and $\{i\} \cup \mathcal{N}_2(i)$ to the second) but in a trivial way as connections between the two “types” of nodes are very sparse, indicating rather a random organization, or at least such a structure cannot be interpreted as compelling evidence of complementarity.

Note that the proposed measures of structural complementarity are based on strong, chordless quadrangles and therefore are different from alternatives such as those proposed in Ref. [27], where authors used a weak definition of quadrangles allowing for any number of chords. This is important as only strong quadrangles lead to definitions which can be interpreted strictly in terms of dense locally bipartite structures and this, as we argue, is crucial for measuring complementarity-driven relations.

Furthermore, when applied to purely bipartite networks the quadrangle-based measures can be seen as variations of the bipartite clustering coefficient(s) [35, 43, 58]. However, the crux is that in our approach quadrangle-based complementarity coefficients can be also applied to unipartite networks in order to quantify jointly local bipartiteness and density, which together are indicative of complementarity-driven relations.

2.2.1. Edge-wise complementarity and structural equivalence

Structural complementarity may be measured also at the level of edges (Fig. 2G). The edge-wise coefficient is defined as:

$$c_{ij} = \frac{2Q_{ij}}{q_{ij}^W + q_{ij}^H} \quad (10)$$

where Q_{ij} is the number of (strong) quadrangles including nodes i and j , q_{ij}^W is the number of (j, i, k, l) and q_{ij}^H of (i, j, k, l) quadruples. Again, $Q_{ij} = Q_{ji}$ and $q_{ij}^W = q_{ji}^H$ so c_{ij} is symmetric.

This way c_{ij} can be seen as a joint measure of bipartiteness around an (i, j) edge and structural equivalence between i and 1-hop neighbors of j and *vice versa*. This way c_{ij} measures the extent to which $N_2(i) \approx N_1(j)$ and $N_1(i) \approx N_2(j)$ without requiring dense connections between the 1-hop and 2-hop neighborhoods of i and j . Note that this is analogous to edge-wise similarity which measures only the extent to which $N_1(i) \approx N_1(j)$ without considering the density of connections between the neighbors of i and j as this would be a higher-order property unrelated to whether an edge is driven by similarity or not (see Figs. 3A and 3B for details).

The formal connection between complementarity and structural equivalence is somewhat more complicated than in the case of similarity and we need to introduce one additional quantity. For a connected triple (k, i, j) we define *Asymmetric Excess Sørensen Index*:

$$H_{kj|i} = \frac{n_{jk} - 1}{d_k - 1 - a_{jk}} \quad (11)$$

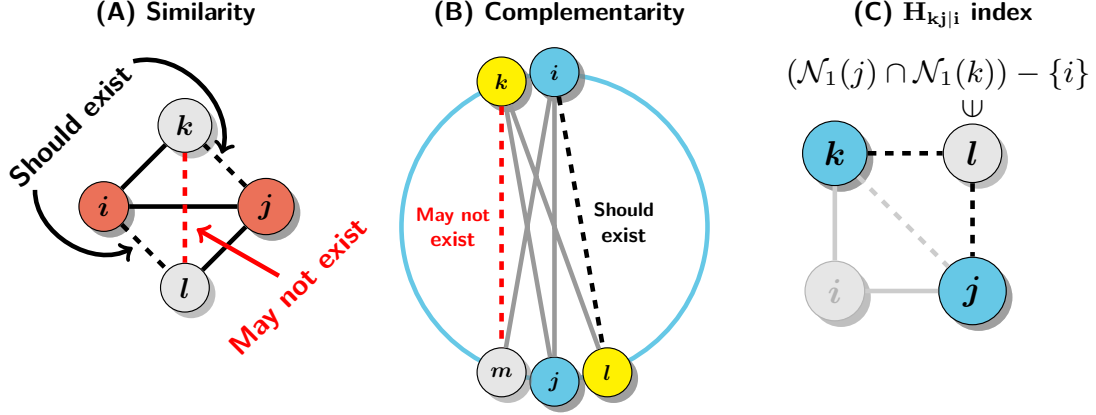


Figure 3. Interpretation of the edge-wise structural coefficients and Asymmetric Excess Sørensen Index. **(A)** If (i, j) edge is driven by similarity then any neighbor of either i or j (k and l on the figure) should be near i (or j) in the latent space making it likely that it links to the other member of the (i, j) pair too. On the other hand, k and l may still be quite far away so the link between them may not exist. **(B)** If (i, j) edge is driven by complementarity then any 2-hop neighbor of j (i), such as l (k) on the figure, should be a 1-hop neighbor of i (j). On the figure the quadruple (i, j, k, l) corresponds to such a situation. On the other hand, any pair of neighbors of i and j correspondingly may be located in the latent space close enough to each other as to make a tie between them unlikely (as it happens for nodes m and k on the figure). **(C)** Construction of the Asymmetric Excess Sørensen Index ($H_{kj|i}$) measuring how structurally equivalent is k with respect to j disregarding any direct links between i , j and k .

which measures how structurally equivalent k is with respect to j while disregarding edges (i, k) , (i, j) and (j, k) . Note that the excess degree of k is used in the denominator as the (i, k) link needs to be ignored. Moreover, a_{jk} term accounts for the possible presence of the (j, k) link. Finally, 1 is subtracted from n_{jk} to account for the fact that i is a shared neighbor of j and k (see Fig. 3C).

It is possible to show that $c_{ij} \leq \max_{k,l} (H_{kj|i}, H_{li|j})$ for $k \in \mathcal{N}_1(i) - \{j\}$ and $l \in \mathcal{N}_1(j) - \{i\}$. Moreover, it can be shown that c_i is a weighted average of c_{ij} 's. These two facts jointly imply that for $j \in \mathcal{N}_1(i)$, $k \in \mathcal{N}_1(i) - \{j\}$ and $l \in \mathcal{N}_1(j) - \{i\}$ the following inequality holds:

$$0 \leq c_i \leq \max_{j,k,l} (H_{kj|i}, H_{li|j}) \quad (12)$$

In other words, local complementarity around a node i is bounded from above by the maximum asymmetric structural equivalence between any pair of its neighbors or neighbors of its neighbors and itself. Crucially, this justifies the interpretation in terms of *structural complementarity*. See SM: S2 for the derivation and other details.

2.2.2. Global complementarity coefficient

From the global perspective of an entire network there is of course no difference between wedge and head quadruples. Hence, the global coefficient can be defined simply as:

$$c = \frac{4Q}{\sum_{i,j} (d_i - 1)(d_j - 1) - n_{ij}} \quad (13)$$

where $(i, j) \in E$ and Q is the total number of quadrangles with no chords. The denominator counts the total number of quadruples.

Note that $c = 1$ if and only if the graph as such is fully connected and bipartite. This agrees with the intuition as this is exactly the structure one should expect in a system composed of two classes of elements in which each element in one class is perfectly complementary to every element of the other.

2.3. Structural coefficients in random graphs

In this section we discuss the behavior of structural coefficients in some of the most important random graph models as such results can be used as natural benchmarks against which to compare and calibrate values observed in real-world networks. First, let us note that in the Erdős-Rényi (ER) model [20] the expected global similarity, which is of course equivalent to global clustering, is simply $\mathbb{E}[s] = p$, or equal to the probability that any edge exists. This is a standard result that follows from the fact that for any (i, j, k) triple the closing (i, k) edge always exists with probability p [Sec. 12.4 in 42].

We can use a similar argument to derive the expected value of global complementarity coefficient in the ER model. Let (i, j, k, l) be any connected quadruple. It forms a quadrangle with no chords if and only if the (i, l) edge exists while the (i, k) and (j, l) edges do not. Since all edges in the ER model exist independently with probability p it means that the expected value of global complementarity coefficient is $\mathbb{E}[c] = p(1 - p)^2$.

2.3.1. Correlations with node degrees in configuration models

A natural null model for studying correlations of node-wise coefficients with node degrees is the configuration model in which a particular degree sequence is enforced while apart from that connections are established as randomly as possible [cf. Sec. 13.2 in 42]. In order to describe the qualitative behavior of the node-wise structural similarity and complementarity coefficients we will use the fact that in both cases they are bounded by their corresponding clustering and closure coefficients (cf. Secs. 2.1 and 2.2). In other words, by describing the correlations between node degrees and triangle/quadrangle clustering and closure coefficients we will be able to reveal the range of the possible behaviors of structural coefficients.

First, let us note that it is usually conjectured that t -clustering should generally decrease with node degree [Sec. 8.6.1 in 42]. More recently, it was analytically proven for the family of random networks with power law degree distributions that t -clustering is on average roughly constant for low-degree nodes and then starts to decrease more quickly as node degree grows [53].

On the other hand, the authors of local closure coefficient, or t -closure using our terminology, showed that it is positively correlated with node degree in the configuration model [57]. Thus, these two results together imply that the structural similarity coefficient, s_i , can display rich, also

non-monotonic, correlations with node degree depending on the large-scale structure of a particular network.

We leave analytical study of the analogous properties of q -clustering and q -closure for future work. However, since both types of clustering and closure coefficients are very similar by construction — in the first case the closing link is between two (in)direct neighbors of i while in the second it is between i and one of its (in)direct neighbors — we conjecture that they should display the same qualitative behavior in the configuration model. More concretely, we expect that q -clustering should decrease with node degree, especially for well-connected nodes, and q -closure should increase with node degree. As a result, we also expect that structural complementarity should vary with respect to node degree in various, also non-monotonic, ways.

We validated the above reasoning on a set of four real-world networks from different domains: (1) Jazz collaborations (offline social); (2) Combined friendship network made of 10 samples of ego-nets from Facebook (online social); (3) Reactome or Human Protein Interactome (biological); (4) Internet at the level of Autonomous System (technological) (see Sec. 4.3 for details).

We studied the correlations between various similarity and complementarity coefficients by plotting their averaged values against node degrees using logarithmic binning with base 2. Moreover, we also plotted corresponding averages calculated based on 100 randomized replicates sampled from Undirected Binary Configuration Model (UBCM) (see Sec. 4.4 for details).

As evident in Fig. 4, the general qualitative behavior of all similarity and complementarity coefficients in randomized networks agrees with the theoretical expectations. Both clustering coefficients tend to be either roughly constant or decrease with node degree in randomized networks. Their behavior in real, observed networks is more nuanced, but in most of the cases follows similar correlation patterns, even if the actual observed values of coefficients are very different. Similarly, both closure coefficients tend to increase with node degrees in both randomized and observed networks suggesting that this correlation may be quite universal.

Similarity and complementarity coefficients in randomized networks tend to follow a path more similar to closure coefficients, but the increase for high degree nodes is less pronounced or the coefficients start to decrease slightly. On the other hand, in many of the observed networks they display more complex, non-monotonic behavior. In other words, the analysis strongly suggests that the theoretical expectations discussed earlier are reasonable and capture much of the trends that can be seen in empirical data.

Interestingly, the analysis also points to some potential differences in terms of the importance of similarity and complementarity between different types of networks. Not surprisingly, all observed similarity-related coefficients are much higher than their randomized counterparts in social networks (Jazz collaborations and Facebook ego-nets). On the other hand, the observed values of complementarity-related coefficients are much closer to the expectations based on the configuration model or even significantly lower.

On the other hand, the correlations observed in the interactome network are somewhat different. In particular, all complementarity measures are significantly increased for low-degree nodes suggesting that the peripheries of the network are more dense and bipartite-like than what could be expected by chance. A similar, but much weaker, increase of complementarity can be observed also in the case of the Internet at the level of Autonomous System, which also features low values of similarity coefficients. Thus, the results suggest that relations in biological and technological networks may be driven by complementarity more often than in social networks. This is, of course, a tentative hypothesis which needs to be tested on a richer empirical material. The crux is, it is structural coefficient we propose that facilitate asking such questions.

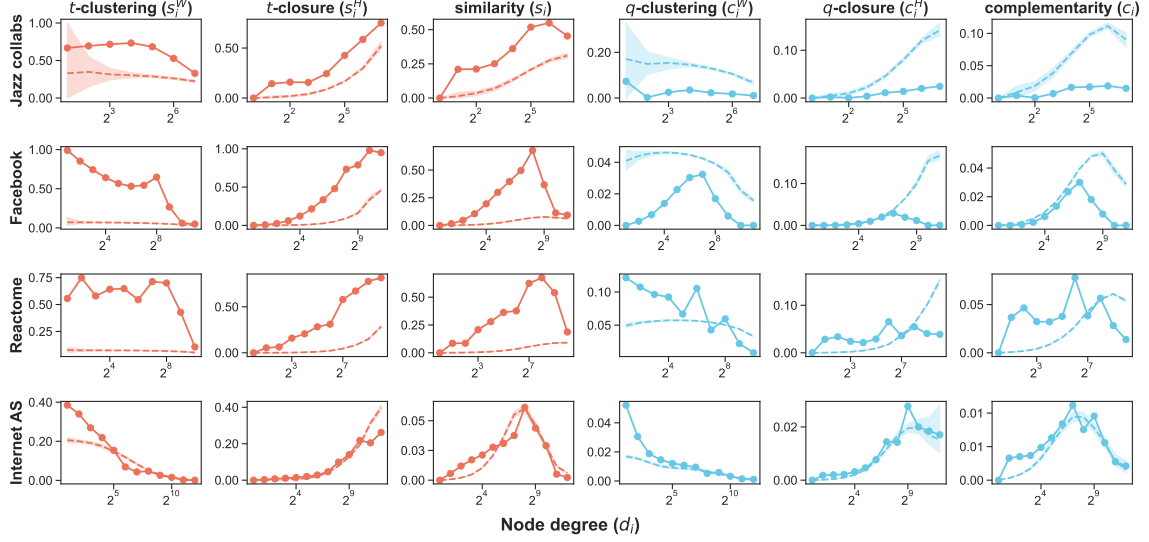


Figure 4. Observed and randomized values of similarity and complementarity coefficients in four real-world networks as a function of node degree agree with the theoretical expectations. Values are averaged in logarithmic bins (with base 2). Dashed lines represent averages based on 100 randomized replicates sampled from Undirected Binary Configuration Model (UBCM) and shaded regions correspond to 95% confidence interval for the null model average.

From a more practical perspective, the analysis indicates that observed values of structural coefficients are usually at least partially constrained by node degrees. Thus, when comparing different networks it is probably best to calibrate the observed values based on a plausible null model such as UBCM in order to account for effects induced purely by the first-order structure (i.e. degree sequences).

2.4. Discriminating between similarity- and complementarity-driven networks

We now turn to the question of the theoretical validity and practical utility of the proposed coefficients. In other words, we want to test whether our measures are related to meaningful, interpretable, domain-specific phenomena.

We test whether structural coefficients can be used to discriminate between different types of social relations. For this purpose, we used a set of (undirected and unweighted) social networks collected by Chami et al. [16] in 17 rural villages in Mayuge District, Uganda. For each village two networks of relations between households were measured: (1) a friendship network and (2) a health advice network (see Sec. 4.3.5 for details).

This dataset provides a perfect opportunity for testing the theoretical validity of our approach as it is sociologically justified to consider the two types of networks as driven by different generating mechanisms. It is a well documented fact that friendship relations are to a large extent driven by homophily, or similarity, between different persons [2, 31, 37, 40]. On the other hand, health

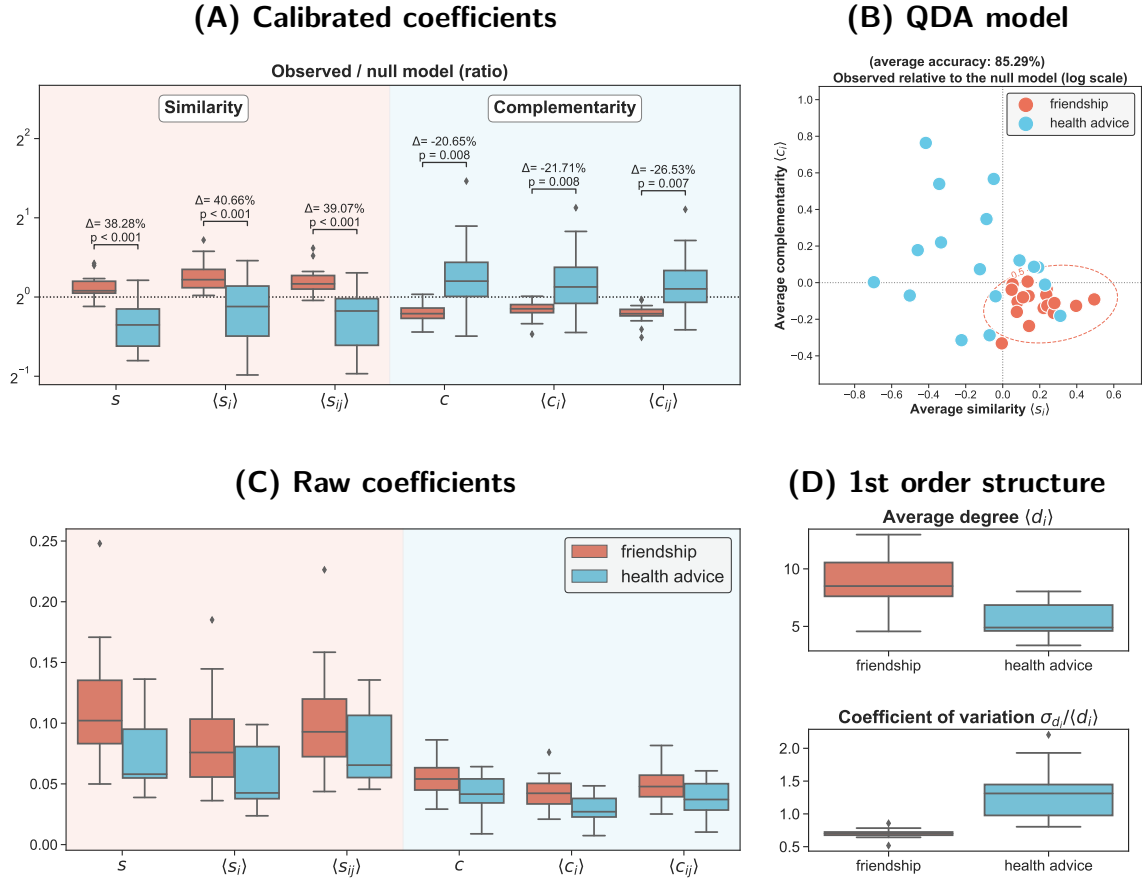


Figure 5. Comparison of structural coefficients between friendship and health advice networks in 17 Ugandan villages. Structural coefficients calibrated against a proper null model accounting for differences in terms of the first-order structure discriminate between friendship and health advice networks. **(A)** Distributions of calibrated coefficients based on 500 samples from UBCM. Effect sizes are expressed in terms of average relative differences between friendship and health advice networks from the same village (Δ). Statistical significance was assessed using one-sample t -test applied to the differences between friendship and health advice networks from the same villages and p -values were adjusted using Holm-Bonferroni method. **(B)** Bivariate distribution of calibrated values of average node-wise similarity and (strong) complementarity coefficients. The decision boundary separating the friendship and health advice networks (marked in red) is based on Quadratic Discriminant Analysis (QDA). **(C)** Distributions of raw coefficients. **(D)** Average first-order structure of the two types of networks as quantified through average degrees and coefficients of variation of degree distributions.

advice networks should be at least partially driven by complementarity, as the act of advice is usually based on a difference in knowledge or information between an adviser and an advisee. More generally, advising can be seen as a particular kind of collaboration, which is known to be linked to complementarity and heterophily [48, 56]. Of course, the structure of the health advice networks can still be expected to be partially influenced by homophily as well as various other processes as

real networks are hardly ever products of a single generating mechanism. However, if the proposed theory is true, there should be some kind of statistical signature of complementarity present in their structure.

In this context it is natural to expect that both global as well as average node- and edge-wise similarity coefficients (s , $\langle s_i \rangle$ and $\langle s_{ij} \rangle$) should be typically higher in the friendship networks. On the other hand, the analogous complementarity coefficients (c , $\langle c_i \rangle$ and $\langle c_{ij} \rangle$) should be on average higher in the health advice networks. Moreover, due to substantial differences between degree distributions of the friendship and health advice networks (see Fig. 5D) the main test was based on values calibrated relative to 500 samples from UBCM (see Sec. 4.5).

As evident in Fig. 5A, the results are in clear agreement with the theoretical expectations. The similarity coefficients in the friendship networks were typically increased relative to the null model (log-ratios greater than zero) and the mean differences were statistically significant at $p \leq 0.001$. On the other hand, the results for the complementarity coefficients were exactly opposite and in this case the health advice networks had significantly larger calibrated values with all mean differences significant at $p \leq 0.01$.

Note that the calibration was necessary as raw values of complementarity coefficients are strongly affected by degree sequences. This is evident in Fig. 5C where the results for similarity coefficients agree with the calibrated analysis while for complementarity they do not. This should not be surprising as quadrangles are higher-order motifs compared to triangles (they consist of 4 instead of 3 nodes) and therefore are more likely to be distorted in noisy, real-world networks. This is why calibration is often necessary when comparing different networks.

In summary, the results confirm that similarity- and complementarity-driven networks have specific structural signatures which can be statistically detected. In order to gauge the discriminatory power of the coefficients better, we fitted also a simple supervised classifier based on Quadratic Discriminant Analysis (QDA) [Sec. 4.3 in 24]. To facilitate visualization we used only two predictors: average node similarity and complementarity coefficients. The out-of-sample accuracy of the model estimated with 17-fold stratified cross-validation (one fold per village) was 85.29% (see Fig. 5B), which provides further confirmation of the theoretical validity of our approach.

3. Discussion

Starting from very general geometric arguments we linked two fundamental relational principles of similarity and complementarity to their characteristic network motifs, that is, triangles and quadrangles correspondingly, and formulated a comprehensive quantitative framework for measuring the extent to which they shape relations in networks. While similarity and its connections to homophily, triadic closure and the density of ego-nets are well-known [31, 32, 50, 57], the principle of complementarity has not been studied systematically from the network perspective. Here we showed that it is linked to the abundance of quadrangles (4-cycles) and the presence of locally dense bipartite-like subgraphs. In other words, both similarity and complementarity leave statistically detectable structural signatures which allow for assessing the degree to which they shaped the structure of any given network.

To formalize our analysis we have introduced two general families of graph-theoretical coefficients for measuring the extent to which relations are driven by similarity or complementarity that can be calculated at the level of edges, nodes and entire graphs. They can be applied to undirected and unweighted networks and are defined in purely combinatorial manner, that is, in terms of counts of

different kinds of paths (triples and quadruples) and cycles (triangles and quadrangles). However, they are motivated by geometric arguments which can be used to extend models developed within the emerging field of network geometry (see Ref. [9] for a recent overview) to systems driven not only by similarity but also complementarity. Indeed, the present work stemmed from our considerations of network geometry going beyond the principle of homophily [40] and we hope that it will prove to be of value in informing a new generation of latent space models.

Even more importantly, by proposing a quantitative network operationalization of the principle of complementarity, our work opens up new possibilities for research on the structure and origins of real-world networks. In particular, our measures of complementarity provide novel tools relevant for studies on systems shaped by collaboration, division of labor and, more generally, heterophily [48, 56].

While we are aware of the complexities associated with the term “structural” in the general network science literature, for instance in the context of graph or node distance/similarity metrics (see Refs. [23, 49] for an overview of these rich topics), we still argue that the measures we propose can be meaningfully called *structural coefficients*. We think so for two reasons: (1) they are defined mathematically purely in terms of observable network structure or without any reference to node or edge attributes (observed or latent); (2) as we show in Secs. 2.1.1 and 2.2.1 they are directly linked to the fundamental notion of structural equivalence [42, 54]. In other words, they really measure the extent to which the structure at the level of a given edge, node or graph is driven by similarity or complementarity.

The proposed family of structural similarity coefficients is built on top of classical local clustering [55] and more recent local closure [57] coefficients. Crucially, it combines these two perspectives in one general measure which captures two different aspects of the fundamental triadic closure process: (1) the tendency of “friends” of ego to connect to each other and (2) the analogous tendency of ego to connect to “friends of its friends”. Moreover, as we show, structural similarity at the level of a node is maximal if and only if the node belongs to a fully connected network. This links our notion of structural similarity directly to a classical result from structural balance theory, namely, the discovery that for a network to be perfectly clusterable it either has to be fully connected or decomposed into multiple fully connected components [18]. In other words, this suggests that too strong a pressure on structural similarity, assuming fixed average degree, must inevitably lead to a decomposition of a system into disconnected parts. We believe that this result may be useful for studies on polarization and social fragmentation [6, 47].

On the other hand, the family of complementarity coefficients, based on counting quadrangles instead of triangles, can be used to measure how dense and bipartite-like are networks at different levels. When limited to the domain of purely bipartite graphs the coefficients can be viewed simply as variations of bipartite clustering coefficient(s) [35, 43, 58]. However, the crux is that the distinction between purely unipartite and bipartite networks is often too sharp and, we argue, network science needs measures for quantifying local bipartiteness. But this should not be done by simply checking whether a given subgraph is bipartite-like, as tree-like subgraphs are also bipartite-like. Instead, a proper measure should account for both bipartiteness and density in order to rule out simpler tree-like structures and this is exactly what is captured by structural complementarity coefficients. Crucially, since bipartite networks are composed of two distinct kinds of entities with connections going only between them, they are complementarity-driven systems *par excellence*. This justifies the interpretation of our coefficients in terms of structural complementarity.

The connection between complementarity and bipartiteness implied by structural coefficients emerges naturally also in other contexts such as games on graphs. One of many types of games

studied in game theory are so-called complementarity games which are used to model problems with negative externalities, that is, such in which the higher the number of players choosing a particular strategy the lower the payoff. Remarkably, it has been shown that if a complementarity game is played on a bipartite graph the equilibrium does not depend on the payoffs associated with different strategies. It is fully determined by the structure of the network [15]. This result not only validates our analysis which links complementarity and bipartiteness but also suggests that complementarity-driven relations may be characteristic for systems and processes characterized by negative externalities (e.g. specialization of countries within the international trade network). This suggests new exciting possibilities for research on links between observable structure of various systems and the principle of complementarity.

Furthermore, we studied the expected values of structural coefficients and their correlations with node degrees in some of the most fundamental random graph models and compared the results to trends observed in several real-world networks from different domains. Our analysis suggests that the presence of complementarity-driven ties may be stronger among low-degree nodes in biological and technological networks than in social networks, which in general do not feature dense bipartite-like subgraphs. The results indicate that more systematic studies of the importance of similarity and complementarity in different types of networks may yield some interesting insights into connections between the structure of networks and their underlying generating mechanisms.

Crucially, we demonstrated that structural coefficients are related to meaningful domain-specific phenomena. We showed that they can be used to discriminate with high accuracy between friendship and health advice networks where the former feature increased structural similarity and the latter increased complementarity.

Last but not least, we designed an efficient algorithm for calculating structural coefficients which can be viewed as a special case of the state-of-the-art graphlet counting method [1] (see Sec. 4.1). The algorithm, together with a suite of auxiliary methods, will be distributed as a Python package through *Python Package Index* upon publication.

An important limitation of our work is the fact that our methods currently can be applied only to undirected and unweighted networks. However, generalizing them to the weighted case should be rather straightforward and we plan to address this problem in the future. In particular, it should be possible to define weighted structural coefficients in the same way as Barrat et al. [7] defined weighted clustering coefficient. On the other hand, the geometric motivation of structural coefficients as well as most of latent space models are inherently undirected, so it is not immediately clear how directed coefficients could be defined. For now, we leave it as an interesting open problem.

4. Materials and methods

4.1. Computing structural coefficients

Structural coefficients are based on counting triples and triangles (similarity) as well as quadruples and quadrangles (complementarity). While the first problem is relatively easy and efficient methods for solving it are implemented in most of popular libraries for graph-theoretical computations, the second problem of counting quadruples and quadrangles is more difficult and corresponding efficient algorithms are not widely known. Here we solve both problems by counting all motifs of interest at the level of individual edges and then aggregate the edge-wise counts to node-wise or global counts when necessary. We propose an algorithm which can be seen as a special case of the state-of-the-art graphlet counting method proposed in Ref. [1]. Pseudocode for the algorithm is presented in

SM: S3.1. We call it **PathCensus** algorithm as ultimately it counts how often different types of paths and cycles occur in a given network.

Node and global counts can be obtained by aggregating edge counts. The rules of aggregation are summarized in Table 1. Table S1 in SM presents detailed formulas for all structural coefficients expressed in terms of the aggregated counts.

Table 1. Notation summary and formulas for aggregating from edge to node and global counts

	Edge	Counting level	
		Node	Global
Paths			
Wedge triples	t_{ij}^W	$t_i^W = \sum_j t_{ij}^W$	$t^W = \frac{1}{2} \sum_{i,j} t_{ij}^W$
Head triples	t_{ij}^H	$t_i^H = \sum_j t_{ij}^H$	$t^H = \frac{1}{2} \sum_{i,j} t_{ij}^H$
Wedge quadruples	q_{ij}^W	$q_i^W = \sum_j q_{ij}^W$	$q^W = \frac{1}{2} \sum_{i,j} q_{ij}^W$
Head quadruples	q_{ij}^H	$q_i^H = \sum_j q_{ij}^H$	$q^H = \frac{1}{2} \sum_{i,j} q_{ij}^H$
Cycles			
Triangles	T_{ij}	$T_i = \frac{1}{2} \sum_j T_{ij}$	$T = \frac{1}{6} \sum_{i,j} T_{ij}$
Quadrangles	Q_{ij}	$Q_i = \frac{1}{2} \sum_j Q_{ij}$	$Q = \frac{1}{8} \sum_{i,j} Q_{ij}$
Structural coefficient	(clustering, closure)		
Similarity	s_{ij}	$s_i \quad (s_i^W, s_i^H)$	s
Complementarity	c_{ij}	$c_i \quad (c_i^W, c_i^H)$	c

4.2. pathcensus package

We implemented all the methods and algorithms for calculating structural coefficients as well as several other utilities including most appropriate null models and auxiliary methods for conducting statistical inference in **pathcensus** package for Python. The core routines are just-in-time compiled to highly optimized C code using *Numba* library [34] ensuring high efficiency. The package has an extensive documentation including several usage examples. It will be distributed through *Python Package Index* upon publication.

4.3. Network datasets

All network datasets used in this paper were obtained from the Netzschleuder network catalogue and repository [45]. In all analyses only largest connected components were used and networks were simplified by removing multilinks and self-loops. Individual network datasets are described below and their unique names within the repository are provided in the following subsection headings. Each dataset can be accessed via a generic link of the form: **networks.skewed.de/net/<name>** where **<name>** is a placeholder which should be substituted with the name of a specific dataset.

Main descriptive statistics for the network datasets (calculated on the giant components) are listed in the corresponding tables in Supplementary Materials (SM).

4.3.1. Facebook ego-network (ego_social)

The network ($n = 4039$, $m = 88234$) is a combination of 10 ego-nets sampled from Facebook [38]. The network is undirected and unweighted.

4.3.2. Jazz collaborations (jazz_collab)

This is an undirected and unweighted network ($n = 198$, $m = 2742$) of collaborations between jazz musicians and bands performing between 1912 and 1940 [22].

4.3.3. Joshi-Tope human protein interactome (reactome)

A network of human proteins and their binding interactions, extracted from Reactome project ($n = 6327$, $m = 147547$). Nodes represent proteins and an edge represents a binding interaction between two proteins [28].

4.3.4. Internet at the level of Autonomous System (internet_as)

A symmetrized snapshot of the structure of the Internet at the level of Autonomous Systems (AS), reconstructed from BGP tables posted by the University of Oregon Route Views Project ($n = 22936$, $m = 48436$). This snapshot was created on 22 July 2006 [29].

4.3.5. Ugandan village networks (ugandan_village)

The dataset consists of unweighted and undirected networks of friendship and health advice relations between households in 17 rural villages bordering Lake Victoria in Mayuge District, Uganda. It has been collected and originally studied by Chami et al. [16]. Relations were measured using the name generator approach in which a representative of each household was asked to indicate up to 10 persons considered friends or trustworthy in regard to health issues. Resulting ties were symmetrized.

4.4. Undirected Binary Configuration Model

Observed values of structural coefficients were calibrated based on Undirected Binary Configuration Model (UBCM) [52]. The model induces a maximum entropy probability distribution over undirected and unweighted networks with n nodes constrained to have a specific expected degree sequence.

4.5. Calibrating values of structural coefficients

In the analyses comparing different networks we calibrated observed values of structural coefficients against UBCM in order to account for effects induced purely by the first-order structure (i.e. degree sequences). Such a calibration may be implemented in many different ways, but all reasonable approaches should yield qualitatively comparable results. We explain our method using an example of a calibration of a graph-level statistic such as average node-wise similarity coefficient, $\langle s_i \rangle$.

First, for an observed network G calculate the value of a graph statistic of interest, $x(G)$. Then, sample R randomized replicates G_i 's of the observed network from a chosen null model (e.g. UBCM)

and calculate $x(G_i)$ for $i = 1, \dots, R$. Finally, the calibrated value of $x(G)$ based on R samples from the null model is defined as the average log-ratio of the observed value and the randomized values:

$$\mathcal{C}(x, R)(G) = \frac{1}{R} \sum_{i=1}^R \log \frac{x(G)}{x(G_i)} \quad (14)$$

Acknowledgments

We thank B. Klein and I. Voitalov for an inspiring conversation on complementarity-driven relations few years ago. We also thank M. Talaga for proofreading and M. Biesaga for help with testing the code.

Funding

This work was supported by a grant from Polish National Science Center (*Outline of a network-geometric theory of social structure*, 2020/37/N/HS6/00796).

Author contributions

S.T. and A.N. conceptualized the project. S.T. formulated the mathematical formalism and wrote the related proofs, designed the algorithms and developed their Python implementation in the form of `pathcensus` package. S.T. conducted the data analyses and prepared the figures. S.T. and A.N. wrote the main text together.

Competing interests

The authors declare no competing interests.

Data and materials availability

Data and code needed for reproducing the analyses presented in the paper will be made freely available as a *GitHub* repository and `pathcensus` package will be released at *Python Package Index* upon publication.

References

- [1] Nesreen K. Ahmed, Jennifer Neville, Ryan A. Rossi, and Nick Duffield. 2015. Efficient Graphlet Counting for Large Networks. In *2015 IEEE International Conference on Data Mining*. IEEE, Atlantic City, NJ, USA, 1–10. <https://doi.org/10.1109/ICDM.2015.141>
- [2] Luca Maria Aiello, Alain Barrat, Rossano Schifanella, Ciro Cattuto, Benjamin Markines, and Filippo Menczer. 2012. Friendship Prediction and Homophily in Social Media. *ACM Transactions on the Web* 6, 2 (2012), 1–33. <https://doi.org/10.1145/2180861.2180866>

- [3] Emanuele Aliverti and Daniele Durante. 2019. Spatial Modeling of Brain Connectivity Data via Latent Distance Models with Nodes Clustering. *Statistical Analysis and Data Mining: The ASA Data Science Journal* 12, 3 (2019), 185–196. <https://doi.org/10.1002/sam.11412>
- [4] Aris Anagnostopoulos, Ravi Kumar, and Mohammad Mahdian. 2008. Influence and Correlation in Social Networks. In *Proceeding of the 14th ACM SIGKDD International Conference on Knowledge Discovery and Data Mining*. ACM Press, Las Vegas, Nevada, USA, 7–15. <https://doi.org/10.1145/1401890.1401897>
- [5] Aili Asikainen, Gerardo Iñiguez, Javier Ureña-Carrión, Kimmo Kaski, and Mikko Kivelä. 2020. Cumulative Effects of Triadic Closure and Homophily in Social Networks. *Science Advances* 6, 19 (2020), eaax7310. <https://doi.org/10.1126/sciadv.aax7310>
- [6] Delia Baldassarri and Peter Bearman. 2007. Dynamics of Political Polarization. *American Sociological Review* 72, 5 (2007), 784–811. <https://doi.org/10.1177/000312240707200507>
- [7] A. Barrat, M. Barthélemy, R. Pastor-Satorras, and A. Vespignani. 2004. The Architecture of Complex Weighted Networks. *Proceedings of the National Academy of Sciences* 101, 11 (2004), 3747–3752. <https://doi.org/10.1073/pnas.0400087101>
- [8] Peter M. Blau. 1977. *Inequality and Heterogeneity: A Primitive Theory of Social Structure*. The Free Press.
- [9] Marián Boguñá, Ivan Bonamassa, Manlio De Domenico, Shlomo Havlin, Dmitri Krioukov, and M. Ángeles Serrano. 2021. Network Geometry. *Nature Reviews Physics* 3, 2 (2021), 114–135. <https://doi.org/10.1038/s42254-020-00264-4>
- [10] Marián Boguñá, Dmitri Krioukov, Pedro Almagro, and M. Ángeles Serrano. 2020. Small Worlds and Clustering in Spatial Networks. *Physical Review Research* 2, 2 (2020). <https://doi.org/10.1103/PhysRevResearch.2.023040>
- [11] Marián Boguñá, Fragkiskos Papadopoulos, and Dmitri Krioukov. 2010. Sustaining the Internet with Hyperbolic Mapping. *Nature Communications* 1, 1 (2010), 62. <https://doi.org/10.1038/ncomms1063>
- [12] Marián Boguñá, Romualdo Pastor-Satorras, Albert Díaz-Guilera, and Alex Arenas. 2004. Models of Social Networks Based on Social Distance Attachment. *Physical Review E* 70, 5 (2004), 056122. <https://doi.org/10.1103/PhysRevE.70.056122>
- [13] Pierre Bourdieu. 1986. *Distinction : A Social Critique of the Judgement of Taste*. Routledge. <https://doi.org/10.4324/9780203720790>
- [14] Pierre Bourdieu. 1989. Social Space and Symbolic Power. *Sociological Theory* 7, 1 (1989), 14–25. <https://doi.org/10.2307/202060>
- [15] Yann Bramoulle. 2001. Complementarity and Social Networks. *SSRN Electronic Journal* (2001). <https://doi.org/10.2139/ssrn.1028335>
- [16] Goylette F. Chami, Sebastian E. Ahnert, Narcis B. Kabatereine, and Edridah M. Tukahebwa. 2017. Social Network Fragmentation and Community Health. *Proceedings of the National Academy of Sciences* 114, 36 (2017), E7425–E7431. <https://doi.org/10.1073/pnas.1700166114>

- [17] Seungwha Chung, Harbir Singh, and Kyungmook Lee. 2000. Complementarity, Status Similarity and Social Capital as Drivers of Alliance Formation. *Strategic Management Journal* 21 (2000), 1–22. [https://doi.org/10.1002/\(SICI\)1097-0266\(200001\)21:1<1::AID-SMJ63>3.0.CO;2-P](https://doi.org/10.1002/(SICI)1097-0266(200001)21:1<1::AID-SMJ63>3.0.CO;2-P)
- [18] James A. Davis. 1967. Clustering and Structural Balance in Graphs. *Human Relations* 20, 2 (1967), 181–187. <https://doi.org/10.1177/001872676702000206>
- [19] Kurt Dopfer, Jason Potts, and Andreas Pyka. 2016. Upward and Downward Complementarity: The Meso Core of Evolutionary Growth Theory. *Journal of Evolutionary Economics* 26, 4 (2016), 753–763. <https://doi.org/10.1007/s00191-015-0434-4>
- [20] Paul Erdős and Alfred Rényi. 1959. On Random Graphs I. *Publicationes Mathematicae* 6 (1959), 290–297.
- [21] Alan Page Fiske. 2000. Complementarity Theory: Why Human Social Capacities Evolved to Require Cultural Complements. *Personality and Social Psychology Review* 4, 1 (2000), 76–94. https://doi.org/10.1207/S15327957PSPR0401_7
- [22] Pablo M. Gleiser and Leon Danon. 2003. Community Structure in Jazz. *Advances in Complex Systems* 06, 04 (2003), 565–573. <https://doi.org/10.1142/S0219525903001067>
- [23] Harrison Hartle, Brennan Klein, Stefan McCabe, Alexander Daniels, Guillaume St-Onge, Charles Murphy, and Laurent Hébert-Dufresne. 2020. Network Comparison and the Within-Ensemble Graph Distance. *Proceedings of the Royal Society A: Mathematical, Physical and Engineering Sciences* 476, 2243 (2020), 20190744. <https://doi.org/10.1098/rspa.2019.0744>
- [24] Trevor Hastie, Robert Tibshirani, and Jerome Friedman. 2008. *The Elements of Statistical Learning* (second ed.). Springer.
- [25] Desmond J. Higham, Marija Rašajski, and Nataša Pržulj. 2008. Fitting a Geometric Graph to a Protein–Protein Interaction Network. *Bioinformatics* 24, 8 (2008), 1093–1099. <https://doi.org/10.1093/bioinformatics/btn079>
- [26] Peter D Hoff, Adrian E Raftery, and Mark S Handcock. 2002. Latent Space Approaches to Social Network Analysis. *J. Amer. Statist. Assoc.* 97, 460 (2002), 1090–1098. <https://doi.org/10.1198/016214502388618906>
- [27] Mingshan Jia, Bogdan Gabrys, and Katarzyna Musiał. 2021. Measuring Quadrangle Formation in Complex Networks. *IEEE Transactions on Network Science and Engineering* (2021), 1–1. <https://doi.org/10.1109/TNSE.2021.3123735>
- [28] G. Joshi-Tope. 2004. Reactome: A Knowledgebase of Biological Pathways. *Nucleic Acids Research* 33, Database issue (2004), D428–D432. <https://doi.org/10.1093/nar/gki072>
- [29] Brian Karrer, M. E. J. Newman, and Lenka Zdeborová. 2014. Percolation on Sparse Networks. *Physical Review Letters* 113, 20 (2014), 208702. <https://doi.org/10.1103/PhysRevLett.113.208702>
- [30] Maksim Kitsak. 2020. Latent Geometry for Complementarity-Driven Networks. *arXiv:2003.06665 [cond-mat, physics:physics]* (2020). arXiv:cond-mat, physics:physics/2003.06665

- [31] Gueorgi Kossinets and D. J. Watts. 2009. Origins of Homophily in an Evolving Social Network. *Amer. J. Sociology* 115, 2 (2009), 405–450. <https://doi.org/10.1086/599247>
- [32] Dmitri Krioukov. 2016. Clustering Implies Geometry in Networks. *Physical Review Letters* 116, 20 (2016). <https://doi.org/10.1103/PhysRevLett.116.208302>
- [33] Pavel N. Krivitsky, Mark S. Handcock, Adrian E. Raftery, and Peter D. Hoff. 2009. Representing Degree Distributions, Clustering, and Homophily in Social Networks with Latent Cluster Random Effects Models. *Social Networks* 31, 3 (2009), 204–213. <https://doi.org/10.1016/j.socnet.2009.04.001>
- [34] Siu Kwan Lam, Antoine Pitrou, and Stanley Seibert. 2015. Numba: A LLVM-based Python JIT Compiler. In *Proceedings of the Second Workshop on the LLVM Compiler Infrastructure in HPC - LLVM '15*. ACM Press, Austin, Texas, 1–6. <https://doi.org/10.1145/2833157.2833162>
- [35] Matthieu Latapy, Clémence Magnien, and Nathalie Del Vecchio. 2008. Basic Notions for the Analysis of Large Two-Mode Networks. *Social Networks* 30, 1 (2008), 31–48. <https://doi.org/10.1016/j.socnet.2007.04.006>
- [36] Michael C. Lawrence and Peter M. Colman. 1993. Shape Complementarity at Protein/Protein Interfaces. *Journal of Molecular Biology* 234, 4 (1993), 946–950. <https://doi.org/10.1006/jmbi.1993.1648>
- [37] Peter V. Marsden. 1988. Homogeneity in Confiding Relations. *Social Networks* 10, 1 (1988), 57–76. [https://doi.org/10.1016/0378-8733\(88\)90010-X](https://doi.org/10.1016/0378-8733(88)90010-X)
- [38] Julian McAuley and Jure Leskovec. 2012. Learning to Discover Social Circles in Ego Networks. In *Advances in Neural Information Processing Systems*, Vol. 25. Curran Associates, Inc.
- [39] J. M. McPherson. 2004. A Blau Space Primer: Prolegomenon to an Ecology of Affiliation. *Industrial and Corporate Change* 13, 1 (2004), 263–280. <https://doi.org/10.1093/icc/13.1.263>
- [40] J. M. McPherson, L. Smith-Lovin, and J. M. Cook. 2001. Birds of a Feather: Homophily in Social Networks. *Annual Review of Sociology* 27, 1 (2001), 415–444. <https://doi.org/10.1146/annurev.soc.27.1.415>
- [41] R. Milo. 2002. Network Motifs: Simple Building Blocks of Complex Networks. *Science* 298, 5594 (2002), 824–827. <https://doi.org/10.1126/science.298.5594.824>
- [42] M. E. J. Newman. 2010. *Networks: An Introduction*. Oxford University Press, Oxford, New York.
- [43] Tore Opsahl. 2013. Triadic Closure in Two-Mode Networks: Redefining the Global and Local Clustering Coefficients. *Social Networks* 35, 2 (2013), 159–167. <https://doi.org/10.1016/j.socnet.2011.07.001>
- [44] Fragkiskos Papadopoulos, Rodrigo Aldecoa, and Dmitri Krioukov. 2015. Network Geometry Inference Using Common Neighbors. *Physical Review E* 92, 2 (2015), 022807. <https://doi.org/10.1103/PhysRevE.92.022807> arXiv:1502.05578

- [45] Tiago P. Peixoto. 2020. The Netzscheuler Network Catalogue and Repository. <https://networks.skewed.de/>.
- [46] Tiago P. Peixoto. 2022. Disentangling Homophily, Community Structure, and Triadic Closure in Networks. *Physical Review X* 12, 1 (2022), 011004. <https://doi.org/10.1103/PhysRevX.12.011004>
- [47] Tuan M. Pham, Andrew C. Alexander, Jan Korbel, Rudolf Hanel, and Stefan Thurner. 2021. Balance and Fragmentation in Societies with Homophily and Social Balance. *Scientific Reports* 11, 1 (2021), 17188. <https://doi.org/10.1038/s41598-021-96065-5>
- [48] Mark T. Rivera, Sara B. Soderstrom, and Brian Uzzi. 2010. Dynamics of Dyads in Social Networks: Assortative, Relational, and Proximity Mechanisms. *Annual Review of Sociology* 36, 1 (2010), 91–115. <https://doi.org/10.1146/annurev.soc.34.040507.134743>
- [49] Pulipati Srilatha and Ramakrishnan Manjula. 2016. Similarity Index Based Link Prediction Algorithms in Social Networks: A Survey. *Journal of Telecommunications and Information Technology* 2 (2016), 87–94.
- [50] Szymon Talaga and Andrzej Nowak. 2020. Homophily as a Process Generating Social Networks: Insights from Social Distance Attachment Model. *Journal of Artificial Societies and Social Simulation* 23, 2 (2020), 6. <https://doi.org/10.18564/jasss.4252>
- [51] Yu Tian, Sebastian Lautz, Alisdair O. G. Wallis, and Renaud Lambiotte. 2021. Extracting Complements and Substitutes from Sales Data: A Network Perspective. *EPJ Data Science* 10, 1 (2021), 45. <https://doi.org/10.1140/epjds/s13688-021-00297-4>
- [52] Nicolò Vallerano, Matteo Bruno, Emiliano Marchese, Giuseppe Trapani, Fabio Saracco, Giulio Cimini, Mario Zanon, and Tiziano Squartini. 2021. Fast and Scalable Likelihood Maximization for Exponential Random Graph Models with Local Constraints. *Scientific Reports* 11, 1 (2021), 15227. <https://doi.org/10.1038/s41598-021-93830-4>
- [53] Remco van der Hofstad, Johan S. H. van Leeuwen, and Clara Stegehuis. 2018. Triadic Closure in Configuration Models with Unbounded Degree Fluctuations. *Journal of Statistical Physics* 173, 3-4 (2018), 746–774. <https://doi.org/10.1007/s10955-018-1952-x>
- [54] Stanley Wasserman and Katherine Faust. 1994. *Social Network Analysis: Methods and Applications*. Cambridge University Press, Cambridge; New York.
- [55] D. J. Watts and S. H. Strogatz. 1998. Collective Dynamics of ‘Small-World’ Networks. *Nature* 393, 6684 (1998), 440. <https://doi.org/10.1038/30918>
- [56] Wen-Jie Xie, Ming-Xia Li, Zhi-Qiang Jiang, Qun-Zhao Tan, Boris Podobnik, Wei-Xing Zhou, and H. Eugene Stanley. 2016. Skill Complementarity Enhances Heterophily in Collaboration Networks. *Scientific Reports* 6, 1 (2016). <https://doi.org/10.1038/srep18727>
- [57] Hao Yin, Austin R. Benson, and Jure Leskovec. 2019. The Local Closure Coefficient: A New Perspective On Network Clustering. In *Proceedings of the Twelfth ACM International Conference on Web Search and Data Mining*. ACM, Melbourne VIC Australia, 303–311. <https://doi.org/10.1145/3289600.3290991>

- [58] Peng Zhang, Jinliang Wang, Xiaojia Li, Menghui Li, Zengru Di, and Ying Fan. 2008. Clustering Coefficient and Community Structure of Bipartite Networks. *Physica A: Statistical Mechanics and its Applications* 387, 27 (2008), 6869–6875. <https://doi.org/10.1016/j.physa.2008.09.006>

Supplementary Materials

S1. Similarity and structural equivalence

Here we derive the relationship between nodal similarity coefficient s_i and structural equivalence between a node i and its neighbors. First, we show that s_i is a weighted average of node-wise coefficients s_{ij} 's for $j \in \mathcal{N}_1(i)$, that is:

$$s_i = \frac{4T_i}{t_i^W + t_i^H} = \frac{\sum_j (t_{ij}^W + t_{ij}^H) s_{ij}}{\sum_j t_{ij}^W + t_{ij}^H} \quad (\text{S1})$$

Note that Eq. (4) implies that $(t_{ij}^W + t_{ij}^H) s_{ij} = 2T_{ij}$. Moreover, since each triangle including i is shared with two other nodes we have that:

$$\sum_{j \in \mathcal{N}_1(i)} (t_{ij}^W + t_{ij}^H) s_{ij} = \sum_{j \in \mathcal{N}_1(i)} 2T_{ij} = 4T_i \quad (\text{S2})$$

On the other hand, $t_{ij}^W + t_{ij}^H$ is the number of 2-paths traversing the (i, j) edges so it can be written as $t_{ij}^W + t_{ij}^H = d_i + d_j - 2$. Hence, it is easy to see that:

$$\begin{aligned} \sum_{j \in \mathcal{N}_1(i)} t_{ij}^W + t_{ij}^H &= \sum_{j \in \mathcal{N}_1(i)} (d_i + d_j - 2) \\ &= d_i(d_i - 1) + \sum_{j \in \mathcal{N}_1(i)} (d_j - 1) \\ &= t_i^W + t_i^H \end{aligned} \quad (\text{S3})$$

Finally, substituting (S2) and (S3) into (S1) we confirm the desired equality.

Now, we note the relationship between Sørensen Index (normalized Hamming similarity) for connected nodes i and j and s_{ij} (4):

$$H_{ij} = \frac{2T_{ij}}{d_i + d_j} = s_{ij} \frac{d_i + d_j - 2}{d_i + d_j} \quad (\text{S4})$$

Note that the above implies that $H_{ij} < s_{ij}$ for all (i, j) edges for which s_{ij} is defined. And since we established that s_i is a weighted average of s_{ij} 's with $j \in \mathcal{N}_1(i)$ we have that:

$$\min_j H_{ij} < \min_j s_{ij} \leq s_i \leq \max_j s_{ij} = \max_j \left(H_{ij} \frac{d_i + d_j}{d_i + d_j - 2} \right) \quad (\text{S5})$$

which proves inequality (5). Note that for large values of $d_i + d_j$ the above is approximately equivalent to:

$$\min_j H_{ij} < s_i \leq \max_j H_{ij} \quad (\text{S6})$$

In other words, we showed that the similarity coefficient of a node i is approximately bounded between minimum and maximum structural equivalence (Sørensen Index) between itself and any of its neighbors.

S2. Complementarity and structural equivalence

Here we derive the relationship between nodal complementarity coefficient c_i and structural equivalence. We start by showing that c_i is a weighted average of edge-wise coefficients c_{ij} 's for $j \in \mathcal{N}_1(i)$, that is:

$$c_i = \frac{4Q_{ij}}{q_i^W + q_i^H} = \frac{\sum_j (q_{ij}^W + q_{ij}^H) c_{ij}}{\sum_j q_{ij}^W + q_{ij}^H} \quad (\text{S7})$$

Using Eq. (10) we can write $2Q_{ij} = (q_{ij}^W + q_{ij}^H) c_{ij}$. Moreover, each strong quadrangle including a node i is shared with exactly two other nodes. Hence, we have that:

$$\sum_{j \in \mathcal{N}_1(i)} (q_{ij}^W + q_{ij}^H) c_{ij} = \sum_{j \in \mathcal{N}_1(i)} 2Q_{ij} = 4Q_i \quad (\text{S8})$$

Next, note that each 3-path starting at an (i, j) edge defines a unique ordered quadruple of the form (i, j, k, l) or (j, i, k, l) . The first form is counted as a head quadruple of the node i and a wedge quadruple of the node j and in the second case the order is reversed. And since $q_{ij}^W + q_{ij}^H$ is the number of 3-paths starting at the (i, j) edge it must hold that the:

$$\sum_{j \in \mathcal{N}_1(i)} q_{ij}^W + q_{ij}^H = q_i^W + q_i^H \quad (\text{S9})$$

Finally, note that (S8) and (S9) jointly mean that Eq. (S7) must be true. As a result, for $j \in \mathcal{N}_1(i)$ we have that:

$$\min_j c_{ij} \leq c_i \leq \max_j c_{ij} \quad (\text{S10})$$

Now, in order to derive the connection between complementarity coefficients and structural equivalence we need to use the notion of weak quadrangles allowing for any number of chordal edges. Let $W_{ij} \geq Q_{ij}$ be the number of quadrangles with any number of chords incident to the (i, j) edge. We also define weak edge-wise complementarity to be $h_{ij} = W_{ij}/(q_{ij}^W + q_{ij}^H) \geq c_{ij}$. It is easy to see that:

$$W_{ij} = \sum_{k \in \mathcal{N}_1(i) - \{j\}} n_{jk} - 1 \quad (\text{S11})$$

On the other hand, the number of 3-paths starting at the (i, j) edge is:

$$\begin{aligned} q_{ij}^W + q_{ij}^H &= \sum_{k \in \mathcal{N}_1(i) - \{j\}} (d_k - 1) + \sum_{l \in \mathcal{N}_1(j) - \{i\}} (d_l - 1) - 2n_{ij} \\ &= \sum_{k \in \mathcal{N}_1(i) - \{j\}} (d_k - 1 - a_{jk}) + \sum_{l \in \mathcal{N}_1(j) - \{i\}} (d_l - 1 - a_{il}) \end{aligned} \quad (\text{S12})$$

since q_{ij}^W is the number of (j, i, k, l) and q_{ij}^H of (i, j, k, l) quadruples. The second equality comes from the fact that $n_{ij} = \sum_k a_{jk} = \sum_l a_{il}$. Now, we can use the two above results and the Asymmetric

Excess Sørensen Index defined in Eq. (11) to rewrite the weak edge-wise complementarity as:

$$h_{ij} = \frac{\sum_k (d_k - 1 - a_{jk}) H_{kj|i} + \sum_l (d_l - 1 - a_{il}) H_{li|j}}{\sum_k (d_k - 1 - a_{jk}) + \sum_l (d_l - 1 - a_{il})} \quad (\text{S13})$$

As a result we have that:

$$\min_{k,l} (H_{kj|i}, H_{li|j}) \leq h_{ij} \leq \max_{k,l} (H_{kj|i}, H_{li|j}) \quad (\text{S14})$$

Using Eq. (S10) we can write:

$$\min_{j,k,l} (H_{kj|i}, H_{li|j}) \leq h_i \leq \max_{j,k,l} (H_{kj|i}, H_{li|j}) \quad (\text{S15})$$

Finally, since by definition $c_{ij} \leq h_{ij}$ this proves Eq. (12). In other words, we just showed that structural complementarity coefficient defined for a node i is bounded from above by the maximum Asymmetric Excess Sørensen Index between any two of its neighbors or itself and any neighbor of its neighbors. Intuitively, high complementarity can exist only in the presence of high structural equivalence between neighbors of i as well as i and neighbors of its neighbors. Moreover, in the weak case we also have a lower bound of the same nature. We leave a more detailed analysis of the notion of weak complementarity for future work.

S3. Structural coefficients and PathCensus

S3.1. Algorithm

Algorithm S1. PathCensus algorithm. It takes an undirected graph $G = (V, E)$ with $|V| = n$ and $|E| = m$ as input and returns edge-wise counts of wedge and head triples and quadruples as well as triangles and strong quadrangles.

```

1: Initialize empty  $C$ 
2: Initialize  $R$  such that  $R_i = 0 \quad \forall i \in V$ 
3: Let  $D$  be the degree sequence of  $G$ 
4: Initialize  $u = 0$ 
5: for  $e = (i, j) \in E$  do
6:   Set  $u = u + 1$ 
7:   Initialize  $T_{ij}, t_{ij}^W, t_{ij}^H = 0$ 
8:   Initialize  $Q_{ij}, q_{ij}^W, q_{ij}^H = 0$ 
9:   Initialize  $\text{Star}_i, \text{Star}_j, \text{Tri}_{ij} = \emptyset$ 
10:  for  $(k \neq j) \in \mathcal{N}_1(i)$  do
11:    Add  $k$  to  $\text{Star}_i$  and set  $R_k = 1$ 
12:    Set  $t_{ij}^W = t_{ij}^W + 1$ 
13:  for  $(k \neq i) \in \mathcal{N}_1(j)$  do
14:    if  $R_k = 1$  then
15:       $T_{ij} = T_{ij} + 1$ 
16:      Remove  $k$  from  $\text{Star}_i$ , add  $k$  to  $\text{Tri}_{ij}$  and set  $R_k = 3$ 
17:    else
18:      Add  $k$  to  $\text{Star}_j$  and set  $R_k = 2$ 
19:       $t_{ij}^H = t_{ij}^H + 1$ 
20:  for  $(k \neq j) \in \mathcal{N}_1(i)$  do
21:    for  $(l \neq i, j)$  do
22:       $q_{ij}^W = q_{ij}^W + 1$ 
23:      if  $R_k = 1 \wedge R_l = 2$  then
24:         $Q_{ij} = Q_{ij} + 1$ 
25:  for  $k \in \text{Star}_i$  do
26:    Set  $R_k = 0$ 
27:  for  $k \in \text{Star}_j$  do
28:    Set  $q_{ij}^H = q_{ij}^H + D_k - 1$  and set  $R_k = 0$ 
29:  for  $k \in \text{Tri}_{ij}$  do
30:    Set  $q_{ij}^H = q_{ij}^H + D_k - 2$  and set  $R_k = 0$ 
31:  Set  $C_u = (T_{ij}, t_{ij}^W, t_{ij}^H, Q_{ij}, q_{ij}^W, q_{ij}^H)$ 
32: return  $C$ 

```

$\triangleright m \times 8$ array for storing path counts
 $\triangleright n \times 1$ array for keeping track of node roles
 $\triangleright n \times 1$ array
 \triangleright the loop may be parallelized
 \triangleright counts of triangles and wedge and head triples
 \triangleright counts of strong quadrangles and wedge and head quadruples
 \triangleright Empty sets for keeping track of nodes with different roles
 \triangleright This internal nested loop determines computational complexity
 \triangleright Set u -th row of C

S3.2. Calculating counts for reversed edges

Note that in our implementation t_{ij}^W counts the number of (k, i, j) and t_{ij}^H tracks (i, j, k) triples. Thus, we have that $t_{ij}^W = t_{ji}^H$. Similarly, q_{ij}^W counts (j, i, k, l) and q_{ij}^H (i, j, k, l) quadruples, so again we have that $q_{ij}^W = q_{ji}^H$. On the other hand, counts of triangles and quadrangles are symmetric. As a result, for the purpose of counting we can assume that all edges are of the form $i < j$ and still be able to count everything correctly. In other words there is no need to consider each undirected edge twice.

S3.3. Formulas

Table S1 below defines formulas for all structural coefficients. They are expressed in terms of path and cycle counts defined in Table 1.

Table S1. Formulas for structural coefficients based on path and cycle counts

Level	Coefficient	Relational principle	
		Similarity	Complementarity
Edges	Structural	$s_{ij} = \frac{2T_{ij}}{t_{ij}^W + t_{ij}^H}$	$c_{ij} = \frac{2Q_{ij}}{q_{ij}^W + q_{ij}^H}$
Nodes	Structural	$s_i = \frac{4T_i}{t_i^W + t_i^H}$	$c_i = \frac{4Q_i}{q_i^W + q_i^H}$
	Clustering	$s_i^W = \frac{2T_i}{t_i^W}$	$c_i^W = \frac{2Q_i}{q_i^W}$
	Closure	$s_i^H = \frac{2T_i}{t_i^H}$	$c_i^H = \frac{2Q_i}{q_i^H}$
Global ¹	Structural	$s = \frac{6T}{t^W + t^H}$	$c = \frac{8Q}{q^W + q^H}$
	Clustering	$s^W = \frac{3T}{t^W}$	$c^W = \frac{4Q}{q^W}$
	Closure	$s^H = \frac{3T}{t^H}$	$c^H = \frac{4Q}{q^H}$

¹ – All global measures are equivalent.

S3.4. Computational complexity

It is clear from the structure of the three nested loops that the asymptotic worst-case computational complexity of both algorithms is $O(md_{\max}^2)$ where m is the number of edges and d_{\max} is the maximum node degree. This agrees with the analysis presented in Ref. [1]. However, in practice the runtime can be reduced by enforcing that edges are defined to satisfy the condition $d_i \leq d_j$ (note that this can always be done without loss of generality). The impact of this optimization can be quite significant for networks with highly heterogeneous degree distributions. For instance, in the case of the network of Internet at the level of Autonomous System ($n = 22936$; $\langle d_i \rangle = 4.22$; $d_{\max} = 2390$) it yields more than five times shorter computation times on average.

S4. Network datasets: descriptive statistics

Table S2. Descriptive statistics for other network datasets ($N = 4$)

domain	network	s	c	n	S	ρ	$\langle d_i \rangle$	σ_{d_i}	d_{\max}
biological	reactome	0.61	0.05	5973	0.94	0.01	48.81	1.39	855
social (offline)	jazz_collab	0.52	0.02	198	1.00	0.14	27.70	0.63	100
social (online)	facebook_combined	0.52	0.02	4039	1.00	0.01	43.69	1.20	1045
technological	internet_as	0.01	0.00	22963	1.00	0.00	4.22	7.81	2390
Average		0.41	0.02	8293.25	0.99	0.04	31.10	2.76	1097.50

s - global similarity (clustering)

c - global complementarity

n - number of nodes in the giant component

S - relative size of the giant component

ρ - edge density

$\langle d_i \rangle$ - average node degree

σ_{d_i} - coefficient of variation of node degrees

d_{\max} - maximum node degree

Table S3. Descriptive statistics for Ugandan village networks ($N = 34$)

domain	network	s	c	n	S	ρ	$\langle d_i \rangle$	σ_{d_i}	d_{\max}
social (offline)	friendship-1	0.06	0.03	202	1.00	0.03	5.42	0.72	32
	friendship-2	0.11	0.05	181	0.99	0.04	7.60	0.77	44
	friendship-3	0.13	0.06	192	1.00	0.06	11.04	0.74	53
	friendship-4	0.09	0.05	320	1.00	0.04	12.97	0.66	50
	friendship-5	0.12	0.05	184	1.00	0.04	7.83	0.69	30
	friendship-6	0.14	0.07	139	1.00	0.07	9.09	0.68	42
	friendship-7	0.17	0.09	121	1.00	0.11	12.73	0.52	32
	friendship-8	0.06	0.04	369	1.00	0.03	9.50	0.70	58
	friendship-9	0.16	0.06	178	1.00	0.07	12.02	0.78	80
	friendship-10	0.10	0.07	207	1.00	0.05	10.55	0.64	44
	friendship-11	0.09	0.04	250	1.00	0.03	8.50	0.70	44
	friendship-12	0.08	0.05	229	1.00	0.03	7.62	0.86	58
	friendship-13	0.10	0.06	183	1.00	0.05	8.84	0.68	34
	friendship-14	0.15	0.06	124	1.00	0.07	8.47	0.64	36
	friendship-15	0.07	0.04	120	1.00	0.04	4.57	0.70	17
	friendship-16	0.05	0.03	372	1.00	0.02	7.38	0.72	43
	friendship-17	0.25	0.07	65	1.00	0.12	7.91	0.70	31
	health-advice_1	0.05	0.04	187	0.98	0.02	4.61	1.31	60
	health-advice_2	0.06	0.06	170	1.00	0.03	4.64	1.66	70
	health-advice_3	0.08	0.05	185	1.00	0.04	6.90	1.43	78
	health-advice_4	0.06	0.04	316	1.00	0.02	6.61	0.96	72
	health-advice_5	0.09	0.02	166	0.99	0.03	4.65	1.45	70
	health-advice_6	0.06	0.02	131	0.98	0.03	4.34	1.93	75
	health-advice_7	0.14	0.06	121	1.00	0.07	7.82	0.80	46
	health-advice_8	0.05	0.03	361	1.00	0.02	6.85	1.04	84
	health-advice_9	0.10	0.05	173	1.00	0.04	7.20	1.42	98
	health-advice_10	0.13	0.05	204	1.00	0.04	8.04	0.98	71
	health-advice_11	0.05	0.04	234	0.97	0.02	4.50	1.67	85
	health-advice_12	0.04	0.04	218	0.99	0.02	4.90	1.30	79
	health-advice_13	0.06	0.03	157	0.91	0.02	3.64	1.25	51
	health-advice_14	0.11	0.05	120	1.00	0.05	5.43	0.80	26
	health-advice_15	0.06	0.05	117	1.00	0.03	3.35	1.36	34
	health-advice_16	0.04	0.01	349	1.00	0.01	4.94	2.21	152
	health-advice_17	0.13	0.06	63	1.00	0.07	4.63	0.95	28
Average		0.09	0.05	197.29	0.99	0.04	7.21	1.01	56.09

s - global similarity (clustering)

c - global complementarity

n - number of nodes in the giant component

S - relative size of the giant component

ρ - edge density

$\langle d_i \rangle$ - average node degree

σ_{d_i} - coefficient of variation of node degrees

d_{\max} - maximum node degree